ACTA IMEKO
ISSN: 2221-870X
September 2023, Volume 12, Number 3, 1 - 8

ADC low-complexity modelling identification and mitigation of baseband intermodulation distortion with instantaneous frequency dependence

Stanislas Dubois[1,2], Bruno Lelong[2], Jean-Michel Hodé[2], Guillaume Ferré[1], Dominique Dallet[1]

[1] *University of Bordeaux, Bordeaux INP, CNRS, IMS, UMR 5218, Talence, France*
[2] *Thales DMS, Elancourt, France*

ABSTRACT
The linearization of active electronic components such as power amplifier or analog-to-digital-converter (ADC), is a vast subject. Many issues come into play, including behavioural modelling with the selection of a relevant model in terms of accuracy, complexity, identification, and compensation. In this paper we consider an ADC linearization problem, we propose an original low-complexity modelling identification and mitigation of baseband intermodulation distortion with instantaneous frequency dependence. Thus, we introduce a refinement of a power series model by adding a dependence on the variation of the instantaneous frequency of the signal. Based on this, we describe a method suitable for the model calibration using a two-tone signal. We finally present a measurement bench adapted to the calibration of the coefficients of the model, followed by some results of linearization. All the methods presented are intended to be operated in real time in embedded systems and are therefore studied to present very low computational complexities.

Section: RESEARCH PAPER

Keywords: Baseband modelling; intermodulation distortion; identification; mitigation; frequency dependence

Citation: Stanislas Dubois, Bruno Lelong, Jean-Michel Hodé, Guillaume Ferré, Dominique Dallet, ADC low-complexity modelling identification and mitigation of baseband intermodulation distortion with instantaneous frequency dependence, Acta IMEKO, vol. 12, no. 3, article 22, September 2023, identifier: IMEKO-ACTA-12 (2023)-03-22

Section Editor: Jan Saliga, Technical university of Kosice, Slovakia, Jakub Svatos, CVUT Prague, Czech Republic, Platon Sovilj, University of Novi Sad, Serbia

Received January 8, 2023; **In final form** April 28, 2023; **Published** September 2023

Corresponding author: Stanislas Dubois, email: stanislas.dubois@u-bordeaux.fr

1. INTRODUCTION

This paper deals with the baseband modelling of the distortion at the output of a high speed (2.6 GHz) and high resolution (14 bits) commercially available ADC. This ADC features IQ demodulation, filtering and decimation, making it possible to select and reduce the useful frequency band of the signal thus digitized. We will use these capabilities later, and we are therefore interested in modelling distortion on complex signals, at the digitization output and downstream processing stages of the ADC.

The objective is thus to propose a model on a complex analytical signal applicable at the output of the digitization chain (ADC, digital IQ amplitude/phase demodulation, and decimation) suitable for calibration and linearization. Although the targeted application is narrow band here, we propose to take into account the frequency dependence, similarly to a memory effect, with a view to versatility. Finally, these models aim to intervene at the end of the digital chain for practical reasons:

1. limitation in flow due to decimation,
2. energy consumption,
3. ease of implementation.

The targeted application of this work is indeed an embedded application. The models considered must then present a limited complexity, facilitating their identification and the implementation of the linearization.

The behavioural models described in the literature can be divided into two categories. The first one includes models that do not take into account the memory effect or frequency variation, mainly power-series models [1]-[3]. For effective broadband modelling, i.e. when the system to be modelled shows a variation of its distortion with frequency, we turn to the second category of models, those taking into account the memory effect. The most comprehensive model is the Volterra model [4]-[6], and many works relate to the simplification [7], rewriting [8]-[10] and truncation [11], [12], of this model. Volterra model indeed presents a consequent computational complexity. We quote in

particular models derived from the Volterra model, which are the models of Wiener [13]-[15], Hammerstein [16]-[18], as well as combinations and generalizations of these models [19]. These latter models, although presenting reduced computational complexities compared to the Volterra model, can however present a large number of coefficients, depending on the size of the associated filters, and require costly identification methods in terms of computational resources.

Based on the previous comments, we propose an extension of a baseband polynomial model by involving the derivative of the sampled analytical signal, and thus by adding an instantaneous frequency dependence to this model. This writing thus makes it possible to model to a certain extent the variation of the non-linearity with the frequency. This method has been patented in 2015 [20].

This paper is organized as follows. We will first develop the distortion model on an analytical signal, and then add the instantaneous frequency dependence. Afterwards, the identification of these models will be studied, from spectral observations of the distortion of two-tone signals. A measurement bench is then presented, allowing the calibration of our ADC, and finally results of identification and linearization by compensation are shown. This paper is an extended version of [21].

2. MODELLING

Any active analog or mixed system generates distortion spurs on its output. This is called a non-linear system. The simplest model allowing to illustrate this phenomenon is the polynomial model, or power-series model, describing a non-linear distortion. A polynomial model links the real input $x(t)$ of a nonlinear system to its output $y(t)$ by the following relation:

$$y(t) = \sum_{p=0}^{P} a_p x^p(t) \approx x(t) + \sum_{p=2}^{P} a_p x^p(t)\,, \tag{1}$$

with P the order of non-linearity of the system, and the a_p the coefficients of the model. The coefficient of order 0 is an offset ($a_0 \approx 0$), and the 1st order coefficient is the linear gain of the system ($a_1 \approx 1$). The nonlinear distortion is then contained in the high order terms. This separation in the distorted signal between the input signal and a function of distortion depending on the input signal allows a compensation of the defects by subtracting this part of distortion from the signal at the output of the system to be linearized.

2.1. Baseband distortion modelling

We find an expression for distortion defects on an analytical signal in [22]-[24]. This model is described in these papers as coming from the polynomial expansion of the complex envelope of an RF signal: $x_{\mathrm{RF}}(t) = 2\Re[x(t)\, e^{j\,\omega_0\, t}]$, where ω_0 is the pulse of the RF carrier frequency of the signal (using the notation of [22]).

Our distortion model $D(\cdot)$ is based on the order 3 Volterra Baseband Series model, with no memory effect [24]:

$$D^{(3)}(x) = \alpha\, x\, |x|^2\,. \tag{2}$$

This model can be extended to the order $2P+1$ as follows:

$$D^{(2P+1)}(x) = x \sum_{k=1}^{P} \alpha_k |x|^{2k}\,. \tag{3}$$

The model presented so far does not present a frequency dependence, i.e. it does not allow to model a memory effect, being a variation of the non-linear distortion as a function of frequency. This point will be dealt with in the next subsection.

2.2. Adding an instantaneous frequency dependence

We here propose to add a dependence of the distortion on the instantaneous frequency of the signal. This instantaneous frequency will be noted f_i. It is expressed as follows for a sinusoidal signal of natural frequency f_0:

$$x(t) = a\, e^{j\,\psi(t)} \text{ with } \psi(t) = 2\,\pi\, f_0\, t + \phi\,, \tag{4}$$

$$f_i(t) = \frac{1}{2\,\pi}\frac{\partial \psi(t)}{\partial t} = \frac{1}{2\,\pi}\frac{\partial}{\partial t}(2\,\pi\, f_0\, t + \phi) = f_0. \tag{5}$$

The instantaneous frequency of a sinusoidal signal therefore corresponds to its natural frequency, the instantaneous frequency of a signal made up of two tones of the same level, to the average of the frequencies of the two tones.

We have,

$$\frac{x'}{x} = \frac{\frac{\partial x}{\partial t}}{x} = j\,\frac{a\; 2\,\pi\, f_0\, e^{j(2\,\pi\, f_0\, t+\phi)}}{a\, e^{j(2\,\pi\, f_0\, t+\phi)}} = j\; 2\,\pi\, f_0\,. \tag{6}$$

Thus:

$$f_i(t) = \frac{1}{2\,\pi}\Im\left[\frac{x'}{x}\right] = \frac{1}{2\,\pi}\frac{\Im[x' x^*]}{|x|^2}. \tag{7}$$

We therefore propose the following refinement to the 3rd order distortion model, Equation (2):

$$D_i^{(3)}(x) = D^{(3)}(x) + \beta\, f_i\, x\, |x|^2 = x(\alpha + \beta\, f_i)\, |x|^2\,, \tag{8}$$

i.e.

$$D_i^{(3)}(x) = x\left[\alpha\, |x|^2 + \frac{1}{2\,\pi}\beta\, \Im(x' x^*)\right]. \tag{9}$$

2.3. Synoptic view in blocks of the model

This model can be represented by a block diagram view (see Figure 1). The differentiator filter is called h_{D} and its delay is written τ_{D}. It is compensated on the other channels so that the following operations are synchronous. The $\frac{1}{2\,\pi}$ factor of Equation (9) is absorbed here in coefficient β. We can finally see here linearization by compensation, by reconstructing the distortions from the input signal and then subtracting them from the signal. This point will be discussed in section 5.

The following section deals with the identification of the presented models.

3. IDENTIFICATION

The identification of this model is done here from frequency observations of a well-known two-tone CW (Continuous Wave) signal, i.e. whose frequencies are known. The frequency identification of this model follows the work of [25]. This method is suitable for a model calibration phase.

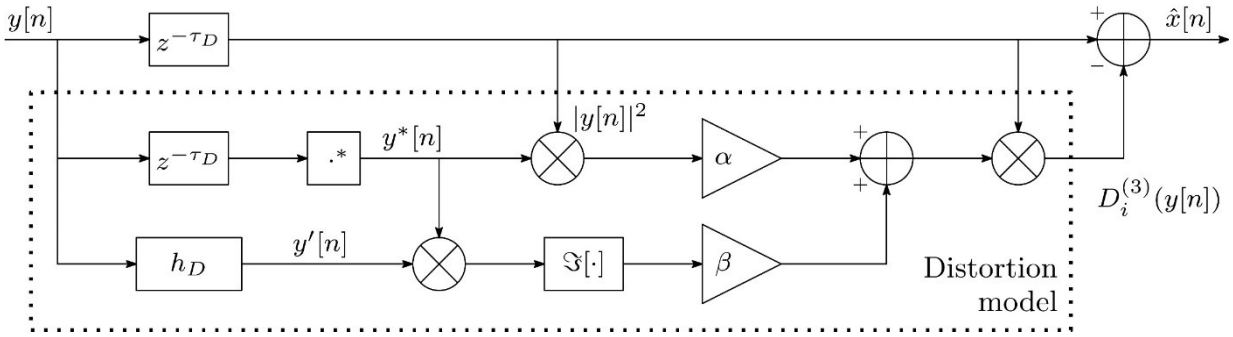

Figure 1. Synoptic model (order 3 with instantaneous frequency dependence) of reconstruction of distortion and compensation.

3.1. Two-tone reference signal

In this paper, we will focus on the response of a commercially available ADC to the excitation of a two-tone signal. This signal used for the calibration of the model, indeed makes it possible to reveal the defects which interest us here, namely the near-carrier inter-modulation. A two-tone signal also has several interesting advantages, an ease in the practical implementation of its generation, and a good coverage of the phase space allowing the excitation of the full dynamic range of the ADC [26]-[29].

For the calibration of the model, we look at the excitation of the ADC by a two-tone signal of the form:

$$x(t) = a_1 e^{j\,2\,\pi\,f_1\,t} + a_2 e^{j\,2\,\pi\,f_2\,t} \tag{10}$$

with a_1 and a_2 the complex amplitudes of the tones of frequencies f_1 and f_2 respectively.

3.2. Identification of the order 3 model with instantaneous frequency dependence

The response of our distortion model with instantaneous frequency to the excitation of a two-tone signal develops as follows:

$$\begin{aligned} y(t) &= x(t) + D_i^{(3)}\big(x(t)\big) \\ &= x(t) + x(t)(\alpha + \beta\, f_i)|x(t)|^2 \\ &= a_1 e^{j\,2\,\pi\,f_1\,t} + a_2\, e^{j\,2\,\pi\,f_2\,t} \\ &+ (\alpha + \beta\, f_i)\,[(a_1^3 + 2\,a_2^2\,a_1)e^{j\,2\,\pi\,f_1\,t} \\ &\quad + (a_2^3 + 2\,a_1^2\,a_2)e^{j\,2\,\pi\,f_2\,t} \\ &\quad + a_1^2\,a_2^*\,e^{j\,2\,\pi\,(2\,f_1 - f_2)t} \\ &\quad + a_1^*\,a_2^2\,e^{j\,2\,\pi\,(2\,f_2 - f_1)t}]\,. \end{aligned} \tag{11}$$

For the identification of the coefficients α and β, we will use the results of two measurements, A and B, around the instantaneous frequencies $f_i^{(A)}$ and $f_i^{(B)}$. These two frequencies will be chosen as the extremities of the band in which the ADC will be modelled.

In our case, the modelling will be performed in a band B_w of a few hundreds kHz to a few MHz, around the RF carrier f_0. We thus have $f_i^{(A)} = f_0 - \frac{B_w}{2}$ and $f_i^{(B)} = f_0 + \frac{B_w}{2}$.

Around these two frequencies $f_i^{(A)}$ and $f_i^{(B)}$, frequencies of fundamental tones 1 and 2 are written $f_1^{(A)}$ and $f_2^{(A)}$ for measurement A, and $f_1^{(B)}$ and $f_2^{(B)}$ for measurement B. Complex amplitudes and phases of the measured tones are written M. Figure 2 summarizes all the notations used for this identification process.

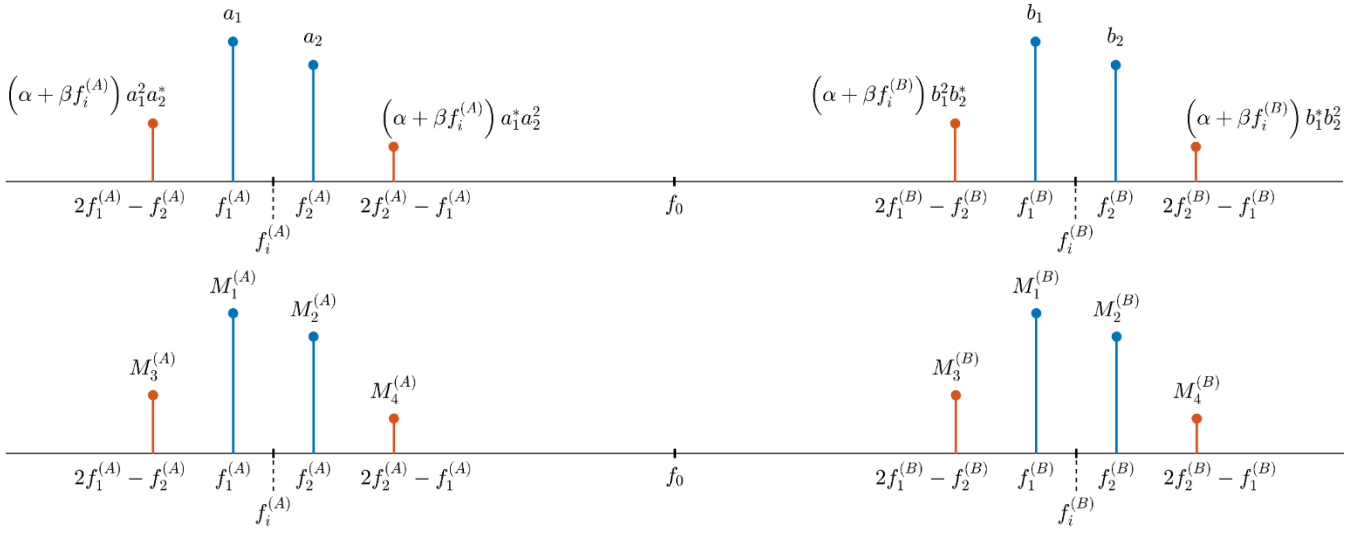

Figure 2. Identification of the order 3 model with instantaneous frequency dependence. Two measurements A and B are performed around instantaneous frequencies $f_i^{(A)}$ and $f_i^{(B)}$ bordering the band of interest, of central frequency f_0. On the top, the output of the model. On the bottom, tones observed on the measurements performed. These measurements are identified to the model output, to retrieve coefficients α and β.

We then have to solve the following system. The coefficients are obtained by averaging a redundant observation of the model:

$$\begin{aligned}\left(\alpha+\beta\, f_i^{(A)}\right) &= \frac{1}{2}\left[\frac{M_{2f_1^{(A)}-f_2^{(A)}}}{M_{f_1}^{2(A)}A_{f_2}^{*(A)}}+\frac{M_{2f_2^{(A)}-f_1^{(A)}}}{M_{f_2}^{2(A)}M_{f_1}^{*(A)}}\right] &= \gamma^{(A)}\\ \left(\alpha+\beta\, f_i^{(B)}\right) &= \frac{1}{2}\left[\frac{M_{2f_1^{(B)}-f_2^{(B)}}}{M_{f_1}^{2(B)}M_{f_2}^{*(B)}}+\frac{M_{2f_2^{(B)}-f_1^{(B)}}}{M_{f_2}^{2(B)}M_{f_1}^{*(B)}}\right] &= \gamma^{(B)}.\end{aligned} \tag{12}$$

This system then resolves to:

$$\begin{aligned}\alpha &= \frac{f_i^{(A)}\gamma^{(B)}-f_i^{(B)}\gamma^{(A)}}{f_i^{(A)}-f_i^{(B)}}\\ \beta &= \frac{\gamma^{(A)}-\gamma^{(B)}}{f_i^{(A)}-f_i^{(B)}}.\end{aligned} \tag{13}$$

For this identification phase, the frequencies of the two tones being known, the instantaneous frequencies $f_i^{(A)}$ and $f_i^{(B)}$ are obtained as follows:

$$\begin{aligned}f_i^{(A)} &= \frac{a_1^2\, f_1^{(A)}+a_2^2\, f_2^{(A)}}{a_1^2+a_2^2}\\ f_i^{(B)} &= \frac{b_1^2\, f_1^{(B)}+b_2^2\, f_2^{(B)}}{b_1^2+b_2^2}\end{aligned} \tag{14}$$

with a_1 and a_2 the complex amplitudes of the two tones of the first measurement, around $f_i^{(A)}$, and b_1 and b_2 the frequencies of the two tones of the second measurement, around $f_i^{(B)}$.

3.3. Identification of the model up to order 7 with no frequency dependence

Order 3 intermodulation brings spurs that are the most powerful in the signal. Intermodulation amplitude then decreases as its order increases. IMD3 therefore is the main defect limiting instantaneous dynamic range. That explains why the first model developed simply was at order 3. There are two reasons for considering a higher order model. The first one is to be able to enhance even further the dynamic range, by also compensating for higher order defects. Once IMD3 is mitigated, the remaining defects limiting dynamic range indeed are intermodulation spurs of higher order. The second reason for considering higher order intermodulation in the model is to take into account the variation of distortion with level [25]. An order 3 model is capable of modelling linear variation of distortion according to input level. An order 5 one models quadratic variation and an order 7 model is able to reproduce cubic variation of distortion with level. The downside is a slight increase in complexity of modelling and identification but more importantly, order 7 defects are harder to identify accurately as they are closer to the noise floor.

The response of an order 7 baseband distortion model, Equation (3) to the excitation of a two-tone signal develops as follows:

$$\begin{aligned}y(t) &= x(t)+D^{(7)}(x(t))\\ &= x(t)+x(t)(\alpha_1|x|^2+\alpha_2|x|^4+\alpha_3|x|^6)\\ &= a_1e^{j2\pi f_1 t}+a_2e^{j2\pi f_2 t}\\ &+ a_1^2\,a_2^*e^{j2\pi(2f_1-f_2)t}[\alpha_1+\alpha_2(2|a_1|^2+3|a_2|^2)\\ &\quad +3\alpha_3(|a_1|^4+2|a_2|^4+4|a_1|^2|a_2|^2)]\\ &+ a_1^*\,a_2^2e^{j2\pi(2f_2-f_1)t}[\alpha_1+\alpha_2(3|a_1|^2+2|a_2|^2)\\ &\quad +3\alpha_3(2|a_1|^4+|a_2|^4+4|a_1|^2|a_2|^2)]\\ &+ a_1^3\,a_2^{*2}\,e^{j2\pi(3f_1-2f_2)t}[\alpha_2+\alpha_3|a_2|^2]\\ &+ a_1^{*2}\,a_2^3\,e^{j2\pi(3f_2-2f_1)t}[\alpha_2+\alpha_3|a_1|^2]\\ &+ a_1^4\,a_2^{*3}\,e^{j2\pi(4f_1-3f_2)t}\,\alpha_3\\ &+ a_1^{*3}\,a_2^4\,e^{j2\pi(4f_2-3f_1)t}\,\alpha_3\end{aligned} \tag{15}$$

with a_1 and a_2 the complex amplitudes of the two tones of respective frequencies f_1 and f_2, and α_1, α_2 and α_3 the parameters of the model.

By identifying the model with the tones at the ADC output (see Figure 3), we get:

$$\begin{aligned}M_1 &= a_1\\ M_2 &= a_2\\ M_3 &= M_1^2\,M_2^*\,[\alpha_1+\alpha_2(2|M_1|^2+3|M_2|^2)\\ &\quad +3\alpha_3(|M_1|^4+2|M_2|^4+4|M_1|^2|M_2|^2)]\\ M_4 &= M_1^*\,M_2^2[\alpha_1+\alpha_2(3|M_1|^2+2|M_2|^2)\\ &\quad +3\alpha_3(2|M_1|^4+|M_2|^4+4|M_1|^2|M_2|^2)]\\ M_5 &= M_1^3\,M_2^{*2}\,[\alpha_2+\alpha_3|M_2|^2]\\ M_6 &= M_1^{*2}\,M_2^3\,[\alpha_2+\alpha_3|M_1|^2]\\ M_7 &= M_1^4\,M_2^{*3}\,\alpha_3\\ M_8 &= M_1^{*3}\,M_2^4\,\alpha_3.\end{aligned} \tag{16}$$

From here, the expression of the coefficients of the model are obtained by inversing the system upwards:

$$\begin{aligned}\alpha_3 &= \frac{1}{2}\left[\frac{M_7}{M_1^4\,M_2^{*3}}+\frac{M_8}{M_1^{*3}\,M_2^4}\right]\\ \alpha_2 &= \frac{1}{2}\left[\frac{M_5}{M_1^3\,M_2^{*2}}+\frac{M_6}{M_1^{*2}\,M_2^3}\right]-\frac{7}{2}\alpha_3(|M_1|^2+|M_2|^2)\\ \alpha_1 &= \frac{1}{2}\left[\frac{M_3}{M_1^2\,M_2^*}+\frac{M_4}{M_1^*\,M_2^2}\right]-\frac{5}{2}\alpha_2(|M_1|^2+|M_2|^2)\\ &\quad -\frac{3}{2}\alpha_3(3(|M_1|^4+|M_2|^4)+8|M_1|^2|M_2|^2).\end{aligned} \tag{17}$$

Going to order 7 here makes it possible to bring precision on the lower orders. Each order of nonlinearity indeed contributes to the lower terms. The terms of order 7 will then present a linear variation with respect to the level, the terms of order 5 will present a quadratic variation, and the terms of order 3, those which interest us the most since limiting the instantaneous dynamic range the most, will present a cubic variation with

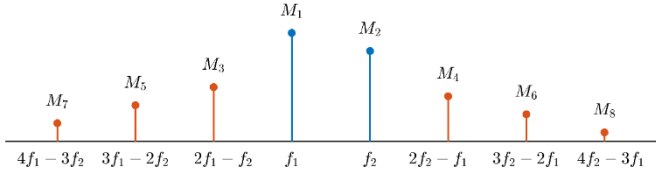

Figure 3. Identification of the order 7 baseband model.

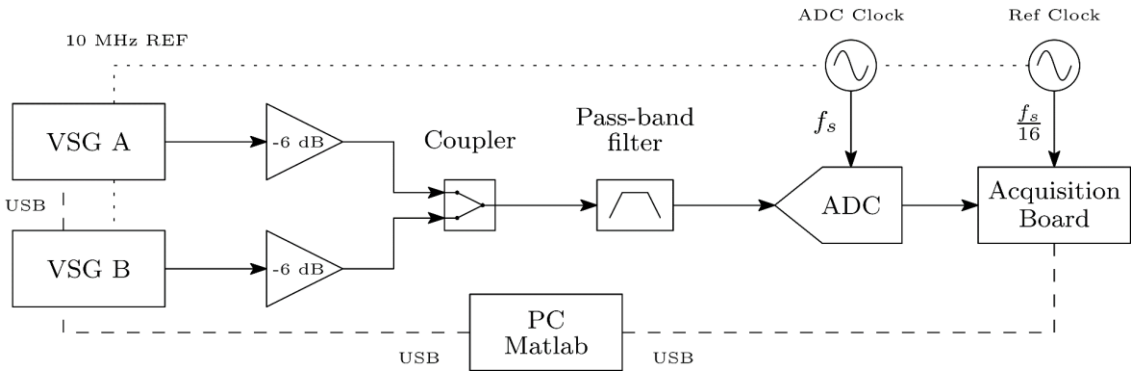

Figure 4. Experimental setup synoptic - f_s is the sampling frequency of the signal.

respect to the level. The modelling of the variation of the distortion tones of order 3 with respect to the level is therefore all the more precise as the order of distortion observed grows.

3.4. Special remark for the identification of the frequency dependence model

When injecting our two-tone signal, Equation (10), in Equation (7), describing the instantaneous frequency from the analytical two-tone signal z, we can develop:

$$\begin{aligned} f_i(t) &= \frac{1}{2\pi}\Im\left[\frac{z'z^*}{|z|^2}\right] \\ &= \frac{f_1+f_2}{2} + \frac{1}{|z|^2}(|a_1|^2-|a_2|^2)\frac{f_1-f_2}{2}\,. \end{aligned} \tag{18}$$

We then find that the instantaneous frequency depends on both the average frequency of the two-tone signal, and on the spacing between the two tones. So that the latter contribution appears in the calculation of the coefficient characterizing the instantaneous frequency, the identification must be carried out at different tones, and with a sufficiently big inter-carrier.

The following section deals with the design of a test-bench suitable for the identification and linearization using previously described methods.

4. EXPERIMENTAL SETUP

In order to validate the theoretical concepts developed in the previous sections, we build the following experimental setup (see the synoptic in Figure 4 and the picture of the bench in Figure 5).

The two-tone signal used as a reference for the calibration is generated by two vector signal generators (VSG A and VSG B). Each sends a CW signal, one at frequency f_1, and the other at frequency f_2, and the two-tone signal is then assembled by a coupler. This signal could be generated by only one of these instruments, but the linearity of the input signal would not be sufficient for the precision required by our measurements. The presence of attenuation in the assembly, between the VSGs and the coupler, also makes it possible to improve the linearity of the reference signal during calibration, by attenuating twice (due to the goings and comings routes), any bounces in the assembly.

A band-pass filter is then used to remove out-of-band noise that can fall back during digitization. Finally, the ADC studied is a commercially available ADC (AD9689, 14 bit, 2.6 Gsps), mounted on its acquisition card. The latter is used to configure the ADC and to recover the points captured at the PC level. Two clock generators are used, one for the ADC clock, and the other for the acquisition card reference clock, for data transfer.

The various measurement and generation instruments are controlled from MATLAB via USB. Finally, all the instruments share the same reference (10 MHz) which allows them to operate synchronously.

The presented identification method is deterministic. The only statistical bias of the identification comes from thermal noise (at signal generation, in the different components, and at digitization). The identification of the parameters of the model is therefore all the more accurate, as the observation of the tones of interest is. This accuracy is harder to obtain as we observe higher orders of distortion. In Fine, the accuracy of the identification lies with the accuracy of the observation of fundamental and spurious tones, meaning their amplitudes relative to the noise floor level.

The following section deals with some linearization results obtained from acquisitions performed using the previously described test-bench.

5. LINEARIZATION

We present in this section linearization results of an ADC using the model, the identification method, and the measurement bench, described in the previous sections.

5.1. Linearization results

To linearize the signal at the output of the ADC from the proposed model, the distortions are reconstructed from the distorted signal itself (see Figure 1). Indeed, the signal is assumed

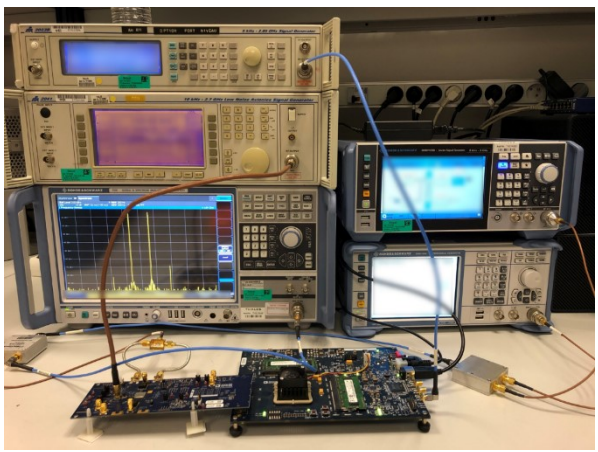

Figure 5. Picture of the experimental setup. On the left from top to bottom, the two clock generators of the ADC and its acquisition card, and the spectrum analyzer. On the right, the two VSGs generating the two tones of the two-tone signal. In the foreground, the ADC on the left, mounted on its acquisition card, on the right.

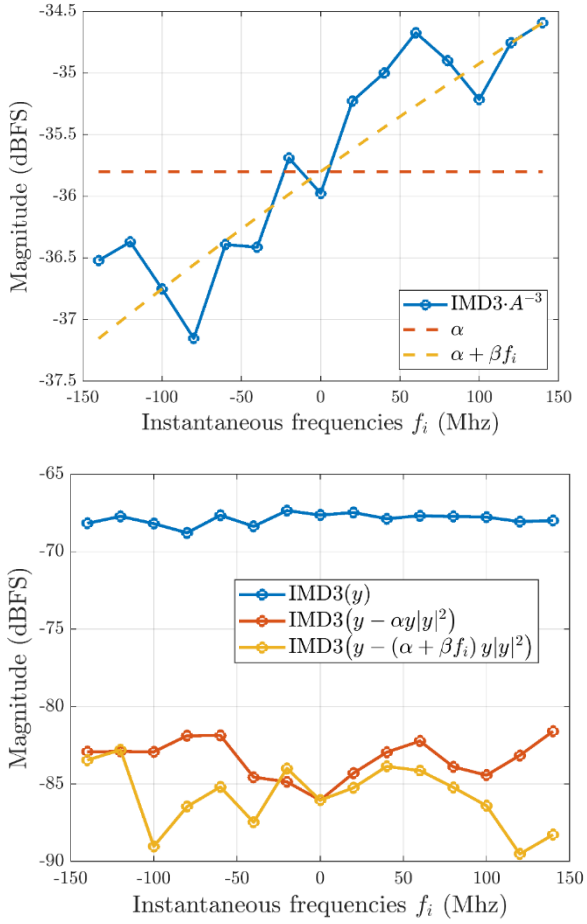

Figure 6. (*top*) Coefficients of order 3 compensation models. A is the magnitude of the fundamentals (assuming they are at the same level). (*bottom*) Linearization results using order 3 compensation models with and without instantaneous frequency dependence.

to be weakly non-linear, that is to say that the parasitic spurs are at a sufficiently low level for their contributions in the reconstruction of the distortions to be negligible.

We thus observe some linearization results in Figure 6, using our order 3 model with instantaneous frequency dependence, and a simply baseband polynomial order 7 model.

These results demonstrate the effectiveness of the compensation with the proposed models. The SFDR (Spurious Free Dynamic Range) is indeed improved up to 27 dB.

5.2. Frequency dependence

To illustrate the relevance and efficiency of the model depending on the instantaneous frequency, we observe the variation of IMD3 (Order 3 intermodulation) in a frequency band. It is then necessary to calibrate the compensation model (here simply to order 3) and note that a simple coefficient α alone cannot translate a variation in frequency of the IMD3, i.e. a memory effect. The instantaneous frequency model is then calibrated on the same band, so as to reproduce this behaviour. The calibrated coefficients and compensation results can be seen in Figure 7.

This model is limited here to a linear variation of the IMD3 as a function of the instantaneous frequency, which can be associated with a narrow band behaviour of the ADC. To model more complex behaviours of the IMD3 with regards to frequency, this model would then have to be extended to a polynomial frequency dependence.

In a band here of about 300 MHz, we observe that for a given level, the IMD3 evolves to a certain extent, linearly with the instantaneous frequency. The proposed model is therefore adapted to the observed behaviour. This is validated by the compensation results in Figure 7. The SFDR is indeed better at the edge of the band, of the order of 6 dB, between the two corrections carried out. The model with instantaneous frequency dependence presents the best results.

This modelling with instantaneous frequency dependence is particularly suitable for modelling ADCs, where the dynamic part of the distortion is partly due to the slew rate limitation. The latter translates into increasingly difficult tracking as the slope of the signal increases, and therefore depends on its rate of variation, or its derivative. The derivative of the signal is finally found in the expression of the instantaneous frequency, see Equation (7), which results in a linear variation of the distortion with the frequency, which we observe in Figure 7.

5.3. Issue with IMD3 dissymmetry

In the results of linearization of Figure 6, a residual distortion can be observed, the compensation of the defects is not total. This is explained in particular by the fact that for two fundamental tones of the same level, the parasitic intermodulation spurs exhibit slight dissymmetries in amplitude. Coming back to the identification method, we have defined the coefficients of the models as being averages of the coefficients that would be obtained by considering only the left or right intermodulation, Equations (12) and (17).

We then show the results of linearizations performed after identification of an order 3 model on either left or right intermodulation tone in Figure 8.

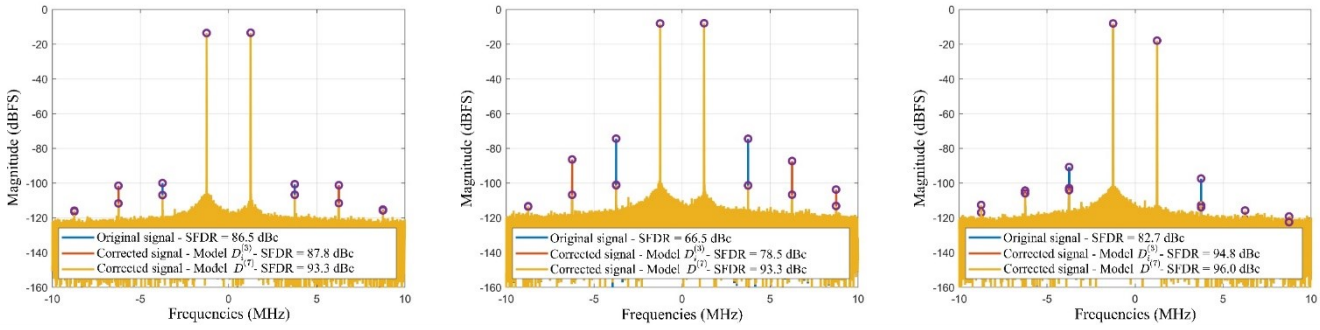

Figure 7. Linearization results with baseband model at order 7 and model with frequency dependence at order 3 – On the left, fundamentals at -12 dBFS both, in the middle, fundamentals at -6 dBFS both, and on the right, fundamentals at -6 dBFS and -16 dBFS.

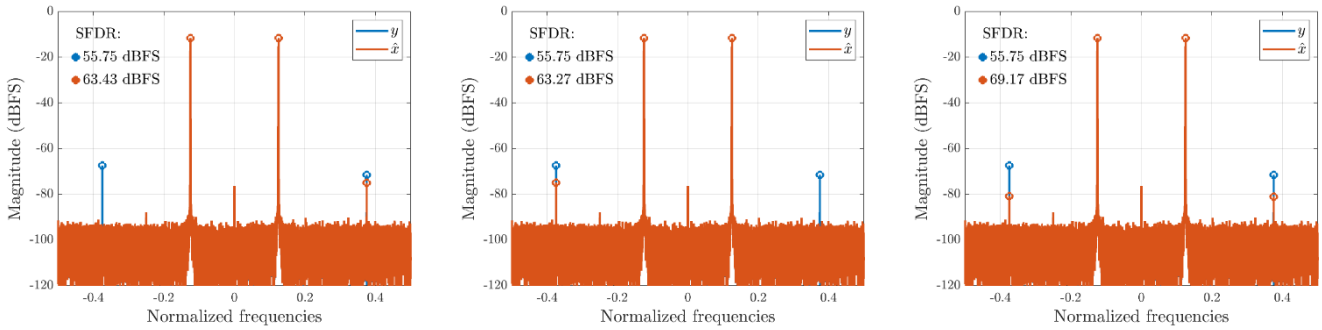

Figure 8. Issue with averaging tones in presence of order 3 intermodulation dissymmetry – On the left, identification performed on the left tone only, in the middle, identification performed on the right tone only, and on the right, identification performed on the average of both intermodulation tones.

On this figure, we indeed observe three linearization results with a model of order 3, thus presenting a single coefficient (see section 2). In the first two cases, the linearization is carried out by identifying the coefficient on the left or right intermodulation product. The correction of this tone is therefore exact, but the overall correction of the signal is penalized, since it is less effective on the other tone. The compromise found therefore corresponds to the last result of Figure 8, where the coefficient of the model is obtained by arithmetically averaging the identifications of the left and right intermodulation products. It is indeed on this result that the SFDR (Spurious Free Dynamic Range) after linearization is the best.

6. CONCLUSION

In this paper, we have presented a baseband distortion model, with an instantaneous frequency dependence, in order to model a nonlinear frequency evolving behaviour. A method for identifying this model, based on a frequency observation of the application of a two-tone signal, is then presented. We finally built a measurement bench adapted to the implementation of the identification of this model.

The results of modelling and linearization present effective mitigation of intermodulation products. The frequency variation of the distortion is modelled by the instantaneous frequency (f_i) dependence.

The main advantage of this model lies with computational complexity of identification (measurements on two-tone signals and FFT) and linearization (only two parameters for this model, and a digital filter to obtain the derivative of the signal). This is valid for narrowband applications where variation of distortion with frequency can be assumed to be linear. Traditional block models such as Wiener, Hammerstein, or combinations and generalizations of these two are much more complex in identification and linearization, but are able to model a richer dependence of distortion relative to frequency, with their combinations of static nonlinearity and filters, more suitable for wideband applications.

When trying to improve the accuracy of the modelling or identifying models going to higher orders, in order to account for higher order intermodulation products, limiting dynamic range, it quickly appears crucial to get out of the noise floor. Indeed, the higher the distortion order observed, the lower the amplitude of the intermodulation products will be, approaching the noise floor. The solution is then to observe on longer time intervals, in order to integrate this measurement noise and to make the noise floor go down spectrally.

To go further, the model with a dependence in instantaneous frequency could be studied for signals more complex than a two-tone signal, not allowing to lift the correlation of the model on a single measurement. One could be inspired by the identification of Volterra kernels from white noise [30].

This method has been studied tested and presented on fast AD converters. Because of its generality, it could be applied to the modelling of other nonlinear systems (amplifiers or other structures of ADCs for example), also presenting this kind of behaviour of their dependence of distortion with frequency.

REFERENCES

[1] J. Tsimbinos, K. V. Lever, Nonlinear system compensation based on orthogonal polynomial inverses, IEEE Transactions on Circuits and Systems 48(4) (2001), pp. 406-417. DOI: 10.1109/81.917978

[2] K. Dogançay, Blind compensation of nonlinear distortion for bandlimited signals, IEEE Transactions on Circuits and Systems 52(9) (2005), pp. 1872 – 1882. DOI: 10.1109/TCSI.2005.852936

[3] P. Nuzzo, F. D. Berardinis, P. Terreni, Efficient polynomial inversion for the linearization of pipeline ADCs, Otranto, Italy, 12-15 June 2006. DOI: 10.1109/RME.2006.1689959

[4] V. Volterra, Sopra le funzioni che dipendono da altre funzioni, 1887 [in Italian].

[5] K. Shi, A. Redfern, Blind Volterra system linearization with applications to post compensation of ADC nonlinearities, IEEE International Conference on Acoustics, Speech and Signal Processing, Kyoto, Japan, 25-30 March 2012. DOI: 10.1109/ICASSP.2012.6288690

[6] J. Tsimbinos, K. V. Lever, Applications of higher-order statistics to modelling, identification and cancellation of nonlinear distortion in high-speed samplers and analogue-to-digital converters using the Volterra and Wiener models, IEEE Signal Processing Workshop on Higher-Order Statistics, South Lake Tahoe, CA, USA, 07 June 1993. DOI: 10.1109/HOST.1993.264531

[7] G. Huang, B. Peng, A. Zhu, Simplified Volterra series based background calibration for high speed high resolution pipelined ADCs, IEEE 58th International Midwest Symposium on Circuits and Systems (MWSCAS), Fort Collins, CO, USA, 02-05 Aug. 2015. DOI: 10.1109/MWSCAS.2015.7282079

[8] G. Favier, T. Bouilloc, Identification de modèles de Volterra basée sur la décomposition PARAFAC, 2009.

[9] M.Herman, B. Miller, J. Goodman, The Cube coefficient subspace architecture for nonlinear digital predistortion, 42nd Asilomar Conference on Signals, Systems and Computers, Pacific Grove, CA, USA, 26-29 Oct. 2008.

DOI: 10.1109/ACSSC.2008.5074750
[10] A. Zhu, J. C. Pedro, T. J. Brazil, Dynamic deviation reduction-based Volterra behavioral modeling of RF power amplifiers, IEEE Transactions on Microwave Theory Techniques 54(12) (2006), pp. 4323-4332.
DOI: 10.1109/TMTT.2006.883243
[11] F. Centurelli, P. Monsurro, F. Rosato, D. Ruscio, A. Trifiletti, Calibration of pipeline ADC with pruned Volterra kernels, Electronic Letters 52(16) (2016), pp. 1370-1371.
DOI: 10.1049/el.2016.1601
[12] B. W. Israelsen, D. A. Smith, Generalized Laguerre reduction of the Volterra kernel for practical identification of nonlinear Dynamic Systems, 2014.
DOI: 10.48550/arXiv.1410.0741
[13] L. Vanbeylen, R. Pintelton, J. Schoukens, Blind maximum-likelihood identification of Wiener systems, IEEE Transactions on Signal Processing 57(8) (2009), pp. 3017-3029.
DOI: 10.1109/TSP.2009.2017001
[14] A. Taleb, J. Sole, C. Jutten, Quasi-nonparametric blind inversion of Wiener systems, IEEE Transactions on Signal Processing 49(5) (2001), pp. 917-924.
DOI: 10.1109/78.917796
[15] P. Liang, S. Guocang, D. Haihua, C. Ming, A Wiener model based post-calibration of ADC nonlinear distortion, IEEE Workshop on Electronics, Computer and Applications, Ottawa, ON, Canada, 08-09 May 2014.
DOI: 10.1109/IWECA.2014.6845633
[16] T. Kowalski, G. P. Gibiino, J. Szewinski, P. Barmuta, P. Bartoszek, P. A. Taverso, Design, characterization, and digital linearization of an ADC analogue front-end for gamma spectroscopy measurements, Acta IMEKO 10(2) (2021), pp. 70-79.
DOI: 10.21014/acta_imeko.v10i2.1042
[17] R. Vansebrouck, C. Jabbour, O. Jamin, P. Desgreys, Fully-digital blind compensation of non-linear distortions in wideband Receivers, IEEE Transactions on Circuits and Systems 64(8) (2017), pp. 2112 - 2123.
DOI: 10.1109/TCSI.2017.2694406
[18] L. Peng, H. Ma, Design and implementation of software-defined radio receiver based on blind nonlinear system identification and compensation, IEEE Transactions on Circuits and Systems 58(11) (2011) pp. 2776–2789.
DOI: 10.1109/TCSI.2011.2151050
[19] M. Schoukens, Block-oriented identification using the best-linear approximation: Benefits and drawbacks, 2017.
DOI: 10.5281/zenodo.291905
[20] J-M. Hodé, Method for correcting intermodulation errors of a conversion circuit, EP3235137, 2015.
[21] S. Dubois, B. Lelong, J-M Hodé, G. Ferré, D. Dallet, Identification and mitigation of intermodulation products using a baseband polynomial distortion model with instantaneous frequency dependence, IMEKO TC-4, Brescia, Italy, 12-14 Sept. 2022.
DOI: 10.21014/tc4-2022.14
[22] M. Grimm, M. Allén, J. Marttila, M. Valkama, R. Thomä, Joint mitigation of nonlinear RF and baseband distortions in Wideband Direct-Conversion Receivers, IEEE Transactions on Microwave Theory and Techniques 62 (2014), pp. 166-182.
DOI: 10.1109/TMTT.2013.2292603
[23] E. Ward, B. Mulgrew, Baseband equivalent Volterra series for modelling cross-channel nonlinear distortion, IEEE Radar Conference, Boston, MA, USA, 22-26 April 2019.
DOI: 10.1109/RADAR.2019.8835647
[24] B. Fehri, S. Boumaiza, Baseband equivalent Volterra series for behavioral modeling and digital predistortion of power amplifiers driven with wideband carrier aggregated signals, IEEE Transactions on Microwave Theory and Techniques 62 (2014), pp. 2594-2603.
DOI: 10.1109/TMTT.2014.2360387
[25] S. Dubois, B. Lelong, J-M. Hodé, G. Ferré, D. Dallet, Frequency identification of a memory polynomial model for PA modeling, IEEE International Instrumentation and Measurement Technology Conference, Ottawa, ON, Canada, 16-19 May 2022.
DOI: 10.1109/I2MTC48687.2022.9806582
[26] P. S. Liam, Y. C. Kuang, M. P-L. Ooi, M. S. Ong, J. C. C. Yeoh, Performance comparison of various multisine excitation signals ADC Testing, Sixth IEEE International Symposium on Electronic Design, Test and Application, Queenstown, New Zealand, 17-19 January 2011.
DOI: 10.1109/DELTA.2011.30
[27] C. L. Monteiro, P. Arpaia, A. C. Serra, Dual tone analysis for phase-plane coverage, ADC Metrological Characterization, Proceedings of the 20th IEEE Instrumentation Technology Conference, Vail, CO, USA, 20-22 May 2003.
DOI: 10.1109/IMTC.2003.1207968
[28] M.S. Ong, Y. C. Kuang, M. P-L. Ooi, S. Demidenko, P. Liam, Optimal dual-tone frequency selection for ADC sine-wave tests, IEEE Transactions on Instrumentation and Measurement 60 (2011), pp. 1533-1545.
DOI: 10.1109/TIM.2010.2102393
[29] J. J. Blair, Selecting test frequencies for two-tone phase-plane analysis of ADCs: Part II, IEEE Transactions on Instrumentation and Measurement 56 (2007), pp. 1171-1175.
DOI: 10.1109/TIM.2007.899910
[30] R. D. Nowak, B. D. Van Veen, Random and pseudorandom inputs for Volterra filter identification, IEEE Transactions on Signal Processing 42 (1994), pp. 2124-2135.
DOI: 10.1109/78.301847